Heteronuclear 2D-correlations in a uniformly [C-13,N-15] labeled membrane-protein complex at ultra-high magnetic fields

Egorova, T.; Hollander, J.G.; Fraser, N.; Gast, P.; Cogdell, R.; Groot, H.J.M. de; ... ; Hoff, A.J.

Journal of Biomolecular NMR, **19:** 243–253, 2001.
KLUWER/ESCOM

Heteronuclear 2D-correlations in a uniformly [^{13}C, ^{15}N] labeled membrane-protein complex at ultra-high magnetic fields

T.A. Egorova-Zachernyuk[a], J. Hollander[a], N. Fraser[b], P. Gast[c], A.J. Hoff[c], R. Cogdell[b], H.J.M. de Groot[a,*] & M. Baldus[a,*,**]
[a]*Gorlaeus Laboratories and* [c]*Huygens Laboratories, Leiden University, 2333 CC Leiden, The Netherlands;* [b]*Division of Biochemistry and Molecular Biology, University of Glasgow, Glasgow G12 8QQ, U.K.*

Received 28 August 2000; Accepted 29 November 2000

Key words: correlation spectroscopy, LH2 light-harvesting complex, MAS, membrane-proteins, photosynthetic bacteria, polarization transfer, spin-diffusion, solid-state NMR

Abstract

One- and two-dimensional solid-state NMR experiments on a uniformly labeled intrinsic membrane-protein complex at ultra-high magnetic fields are presented. Two-dimensional backbone and side-chain correlations for a [U-^{13}C,^{15}N] labeled version of the LH2 light-harvesting complex indicate significant resolution at low temperatures and under Magic Angle Spinning. Tentative assignments of some of the observed correlations are presented and attributed to the α-helical segments of the protein, mostly found in the membrane interior.

Introduction

Structure elucidation of immobilized globular and membrane-proteins using solid-state nuclear magnetic resonance (SSNMR) techniques (Mehring, 1983; Ernst et al., 1987) has made considerable progress (for recent reviews see e.g.: Cross and Opella, 1994; McDowell and Schaefer, 1996; Smith et al., 1996; Griffin, 1998; Marassi and Opella, 1998). Valuable structural information has been obtained on membrane proteins such as rhodopsin (Feng et al., 1997, 2000), bacteriorhodopsin (Thompson et al., 1992), nicotinic acetylcholine and NMDA receptors (Opella et al., 1999), and resulted in the determination of a complete structure in the case of gramicidin A (Ketchum et al., 1993, 1997). So far, stable isotope labeling in conjunction with Magic Angle Spinning (MAS; Andrew et al., 1958) or preferential sample orientation techniques (Cross and Opella, 1994; Sanders et al., 1994; Marassi and Opella, 1998) have been most successful to achieve sensitivity and resolution compulsory for biological SSNMR studies. MAS-based methods have successfully been employed to determine internuclear distances (see e.g. Creuzet et al., 1991; Griffiths et al., 1994; Klug et al., 1997; Benziger et al., 1998; Verdegem et al., 1999) or torsion angles (Feng et al., 1997, 2000; Bower et al., 1999) well beyond the resolution obtainable in X-ray crystallography. Most of these studies involved single or doubly labeled compounds customized for the biophysical problem under study and in close reference to low-resolution structural models. As for example demonstrated in uniformly labeled ^{13}C networks (Boender et al., 1995; Egorova-Zachernyuk et al., 1997), MAS studies involving multiply labeled biomolecules may permit structural investigations with greater flexibility and may profit from residue-specific chemical shift information obtained in the liquid state (Wishart et al., 1991).

A prerequisite for structure determination of partially (Hong and Jakes, 1999; Hong, 1999) or uniformly labeled peptides and proteins (Straus et al., 1998; Nomura et al., 1999; McDermott et al., 2000; Pauli et al., 2001) are hetero- and homonuclear as-

*To whom correspondence should be addressed. E-mail: maba@mpibpc.mpg.de (M.B.); ssnmr@chem.leidenuniv.nl (H.J.M.d.G.)
**Present address: Max-Planck-Institute for Biophysical Chemistry, Am Fassberg 11, D-37077 Göttingen, Germany.

signment techniques. For both aspects, a variety of pulse schemes have been proposed (for recent reviews see e.g. Bennet et al., 1994; Baldus et al., 1998a) and have for example recently been employed for a complete assignment of a uniformly labeled SH3 domain containing 62 residues (Pauli et al., 2001). Partial assignments were also reported for ubiquitin (Straus et al., 1998; Hong, 1999) and BPTI (McDermott et al., 2000). These systems are suitable candidates to establish MAS-based protocols that determine conformations of peptide ligands bound to their membrane-protein receptor target (Pellegrini and Mierke, 1999; Watts, 1999) or structural constraints in globular proteins (Siegal et al., 1999). The number of residues in these peptides also compares favorably to membrane-spanning or surface-bound peptides studied recently in oriented lipid bilayers (see e.g. Marassi et al., 1999; Opella et al., 1999). It can thus be inferred that MAS-based correlation techniques could also be used to study entire membrane-protein topologies or subsections thereof.

In this contribution we are making a next step towards membrane-protein structure elucidation under MAS and show that heteronuclear (^{13}C,^{15}N) correlations of significant resolution can be obtained in a *completely* labeled membrane-protein environment. So far, only a small number of membrane-proteins have been characterized by electron microscopy or X-ray crystallography such as integral membrane light-harvesting complexes from photosynthetic bacteria. These systems represent ideal candidates to examine and improve NMR techniques for applications in multi-labeled membrane-proteins. We have thus chosen a uniformly (^{13}C,^{15}N) labeled version of the LH2 light-harvesting complex from the purple non-sulphur photosynthetic bacterium *Rhodopseudomonas acidophila* 10050 strain (Zuber and Brunisholz, 1993; McDermott et al., 1995). The crystal structure contains three asymmetric units, each including three protomer complexes. These complexes consist of an α- (53 amino acid residues) and β- (41 amino acid residues) apoprotein, three bacteriochlorophyll *a* molecules, one rhodopsin-glucoside carotenoid and a β-octylglucoside detergent molecule. Both proteins have been sequenced (Zuber and Brunisholz, 1993) (Figure 1). The transmembrane helices of nine α-apoproteins are packed side by side to form a hollow cylinder of 18 Å radius. The nine helical β-apoproteins are arranged radially with the α-apoprotein to form an outer cylinder of 34 Å. To our knowledge, the present system (about 150 kDa) represents one of the largest integral membrane-protein complex investigated by NMR so far and we here report on results obtained on a novel wide-bore 750 MHz NMR instrument offering increased resolution and sensitivity compared to standard-size systems.

Material and methods

Uniformly [^{13}C,^{15}N] enriched variants of the LH2 light-harvesting complex were obtained by growing purple photosynthetic bacteria *Rps. acidopila* 10050 anaerobically in light at 30 °C on a well-defined medium containing 2 g/l [U-^{13}C,^{15}N] algae hydrolysate (EMBL, Heidelberg), 1 g/l [U-^{13}C,^{15}N] labeled $(NH_4)_2$-Succinate, 2.7 g/l KH_2PO_4 and 3.4 g/l K_2HPO_4. 20 ml/l of a trace element solution was added to the medium. 0.1 ml/l of a biothine–thiamine solution (containing 0.5 g of thiamine chloride and 8.3 g biothine per 20 ml of vitamin solution, 5% ethanol/water) was included in the medium. 1N HCl was used to adjust the pH of the medium to 5.6. Cultures were grown illuminated with an incandescent light intensity of 1.5 klux. After 17 days of growing, the cells were harvested by centrifugation. After resuspension in 20 mM Tris-HCl, the solution was defrosted and resuspended in 20 mM Tris-HCl at pH 8.0. The LH2 complex was subsequently prepared as described by Hawthorn and Cogdell (1991). The cells were mechanically disrupted using a French Press at a pressure of 15000 psi. Unbroken cells and large membrane fragments were removed by centrifugation for 20 min at 10000 rpm and 4°C. The supernatant with chromatophores was pooled and chromatophores were isolated by centrifugation for 2 h with 55000 rpm at 4 °C. The pellets were resuspended in 20 mM Tris buffer. The membranes were diluted in 20 mM Tris-HCl (pH 8.0) to an A_{859} of 75 before further treatment with 2% (v/v) LDAO during 4 h at 4 °C. Insoluble material was removed by centrifugation prior to application of the supernatant to a sucrose gradient. Using a 36 ml polycarbonate centrifuge tube, 6 ml of solubilized membranes was layered on top of the sucrose and centrifuged at 55000 rpm for 16 h at 4 °C. The LH2 fraction was further purified by gel filtration chromatography, concentrated (70 kDa-filter) to approximately 3 ml and checked by SDS-PAGE with a 12.5% bisacrylamide running gel. Finally, the [U-^{13}C,^{15}N] LH2 complex was characterized by optical absorption spectroscopy.

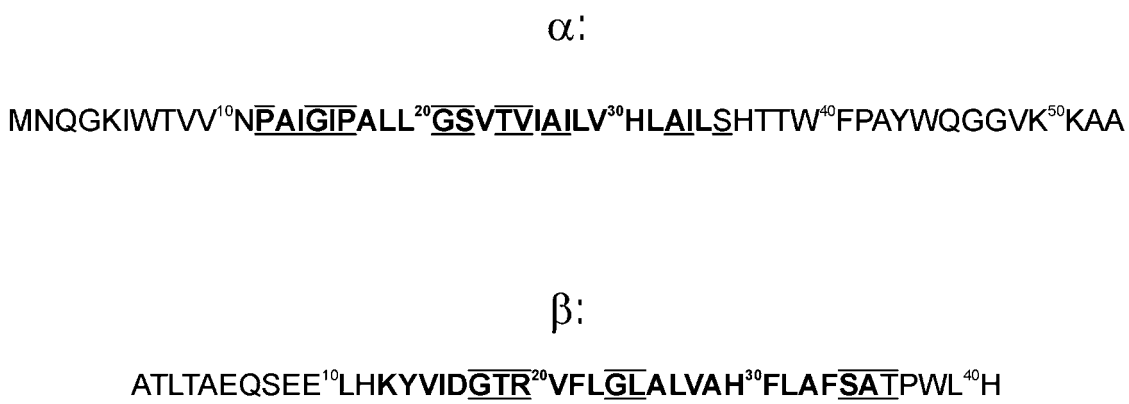

Figure 1. Amino acid sequence for the α and β protein subunits of *Rhodopseudomonas acidophila* 10050 B800–B850. Membrane-spanning residues are indicated in bold. Residue types tentatively identified in this work are underlined. Assigned residues are indicated using an additional line above the letter.

NMR experiments were performed using a MSL 400 and a DSX 750 wide-bore spectrometer (Bruker, Germany). Triple resonance experiments at ultra-high fields were conducted using a 4 mm (^{1}H,^{13}C,^{15}N) triple-channel MAS probe. Solutions of uniformly labeled LH2 samples were concentrated to a volume of 30 μl amounting to 10 mg of protein in a 4 mm CRAMPS rotor. MAS spinning rates between 8 and 12 kHz were used in the temperature range of −10 °C to −50 °C. Stable sample cooling was achieved using a pressurized N_2 heat exchanger/dewar system permitting N_2 refill intervals of longer than 20 h.

Experiments and discussion

1D CPMAS experiments

One-dimensional (^{13}C)-CPMAS (Pines et al., 1973) spectra of [U-^{13}C,^{15}N] labeled LH2 at 750 MHz are shown in Figure 2A. For comparison, results at 400 MHz are included in Figure 2B. Both spectra were recorded at −30 °C using a MAS frequency of 8 kHz and TPPM decoupling (Bennett et al., 1995) during acquisition. Note that the spectrum at ultra-high field was recorded with a significantly smaller number of scans, in agreement with the larger sensitivity of the 750 MHz system. As expected, contributions from spinning sidebands are here more pronounced. On the other hand, the overall resolution increases, in particular visible in the side-chain region of the spectrum. Next we investigate the influence of sample temperature upon resolution and stability of the sample (Figure 3). For each spectrum, NMR hardware settings were carefully optimized. Figure 3 reveals an overall stability of the sample at the indicated temperatures and a slight improvement in resolution for higher temperatures, predominantly observed for the side-chain resonances. These observations are supported by additional 2D experiments that revealed an improved resolution for T = −10 °C. For these reasons, all 2D spectra presented in the following were recorded at −10 °C.

2D (NC) correlation experiments

Methods only involving proton and/or carbon resonances during evolution or detection periods are not likely to provide sufficient resolution with MAS and at low temperature to resolve entire backbone or side-chain networks. To test the degree of resolution and sensitivity obtainable in the system described above we focus in the following on 2D-(^{13}C,^{15}N) correlation experiments. Comparable to the liquid state (Kay et al., 1990; Montelione and Wagner, 1990; Cavanagh et al., 1996), spectral assignment requires in general hetero- and homonuclear transfer steps that direct polarization from one spin to the next in the polypeptide chain in high efficiency. For applications in uniformly labeled globular or membrane-proteins under MAS, the polarization technique employed should fulfill the following criteria: the r.f. scheme should maximize the transfer efficiency and allow for an unambiguous interpretation of correlations in terms of spatial distance without truncation effects or unwanted relay transfer caused by additional hetero- or homonuclear dipolar couplings. In order to avoid signal loss or recoupling during selective pulses, polarization transfer that is inherently chemical shift selective is to be preferred. For ultra-high magnetic field, techniques that can be

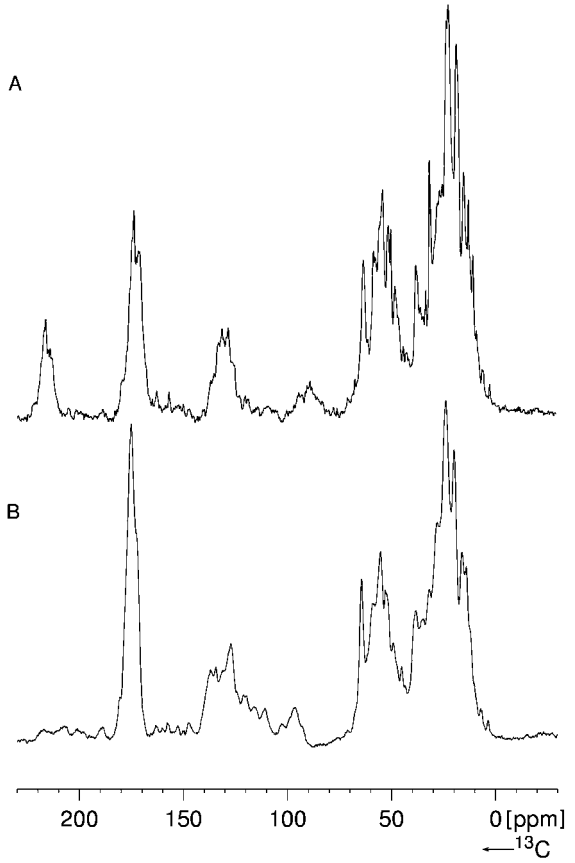

Figure 2. (^{13}C)-CPMAS (Pines et al., 1973) spectra of [U-^{13}C,^{15}N] LH2 recorded with a MAS frequency of 8 kHz at −30 °C at (A) 750 MHz (16 scans) and (B) 400 MHz (256 scans). In all cases, signal intensities were optimized using amplitude modulated ^{13}C r.f. fields (Metz et al., 1994; Hediger et al., 1995) during the (^{1}H,^{13}C) CP transfer step. During acquisition, TPPM (Bennett et al., 1995) proton decoupling at 70 kHz r.f. field strength was applied.

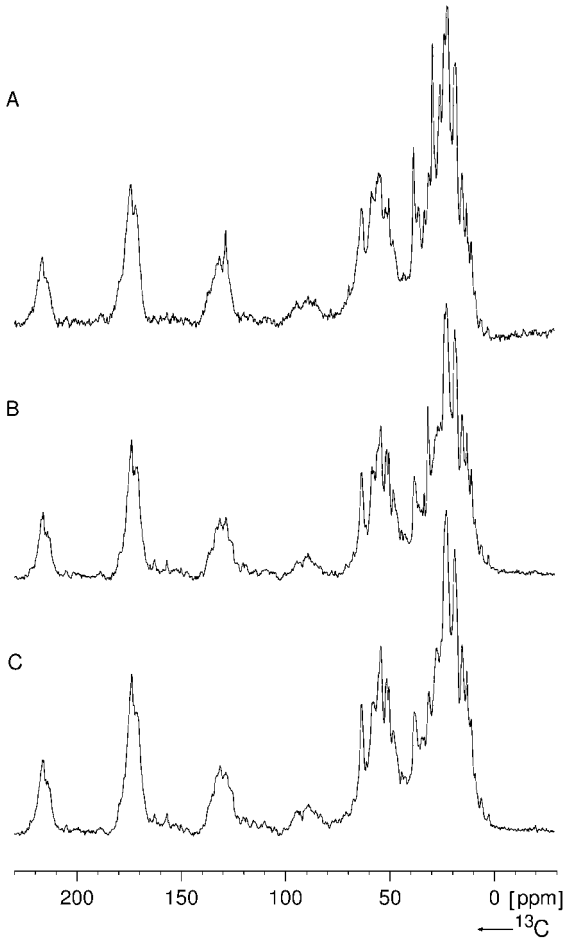

Figure 3. (^{13}C)-CPMAS spectra of [U-^{13}C,^{15}N] LH2 recorded at 750 MHz with a MAS frequency of 8 kHz at different temperatures: −10 °C (A), −30 °C (B), −50 °C (C). R.f. fields during CP and acquisition were optimized for each temperature.

employed at low to medium r.f. field strength and high MAS frequencies are desirable.

For heteronuclear transfer in polypeptides, Baldus et al. (1998b) discuss in detail how the conventional CP (Pines et al., 1973) approach can be modified to direct polarization transfer in a chemical shift selective manner. The usefulness of this approach in the context of uniformly labeled globular (Pauli et al., 2001) and partially labeled membrane-proteins (Petkova et al., to be published) has already been demonstrated. Briefly, zero-quantum (ZQ) polarization transfer for polarization transfer within a heteronuclear I,S spin pair (described by the chemical shift offsets Ω_I and Ω_S) occurs if applied r.f. fields (ω_{1I}, ω_{1S}) and MAS frequency ω_R fulfill a simple algebraic condition ($\sqrt{\Omega_I^2 + \omega_{1I}^2} - \sqrt{\Omega_S^2 + \omega_{1S}^2} = n\omega_R$, with n = 1, 2). Further optimizations that e.g. prevent simultaneous single-quantum recoupling of chemical shielding interactions or establish double-quantum transfer are discussed by Baldus et al. (1998b). Band-selective SPECIFIC CP techniques that fulfill all of the above stated conditions and allow for the observation of NC correlations can be realized by the introduction of a slow amplitude modulation, for instance, on the ^{15}N r.f. channel during a (^{15}N,^{13}C) 2D experiment (Figure 4). Note that the discussed concept achieves polarization transfer and band-selectivity without phase or frequency modulation. It is thus amenable to methodological extensions such as homonuclear decoupling schemes, often essential in macroscopically oriented

systems (Sanders et al., 1994; Marassi and Opella, 1998).

Following the experimental protocol outlined in Figure 4, 2D-(^{15}N,^{13}C) correlations on [U-^{13}C,^{15}N] LH2 are shown in Figure 5. After a broadband HN transfer step, band-selective NC transfer ($\tau(^{15}N,^{13}C) = 2$ ms) was optimized to observe prominent NCO (Figure 5A) and NCA (Figure 5B) correlations. For Figure 5, a MAS frequency of 8 kHz and a temperature of -10 °C were chosen. TPPM decoupling at 85 kHz was applied in t_1 and t_2. SPECIFIC CP (Baldus et al., 1998b) transfer was established using r.f. fields between 10–25 kHz and optimized for an r.f. carrier frequency positioned slightly outside the CO (Figure 5A) and the C_α (Figure 5B) resonance regime. In a total experiment time of about 4 h, 128 t_1 experiments were performed. Additional experimental details can be found in the figure caption.

In the NCO correlation (Figure 5A) 10–15 resolved peaks around a relatively broad, but structured correlation area at 120 ppm (^{15}N chemical shift) can be identified. As expected, the relatively small chemical shift range of carbonyl resonances leads to significant overlap – even in the 2D experiment. In Figure 5B, results of an NCA correlation under identical experimental conditions are shown. In line with NMR studies of proteins in solution (Wishart et al., 1991) and recent SSNMR results on globular proteins (McDermott et al., 2000; Pauli et al., 2001), the increased dispersion in C_α resonances leads to a significant number of resolved resonance lines detectable in the NCA correlation area. Individual peaks with ^{15}N and ^{13}C linewidths of 1.2 ppm and 1 ppm, respectively, are observed. While resolution down to the baseline is only possible for a limited number of these correlations, a total number of about 30–40 peak maxima can be identified. This number is consistent with an observation of the membrane-spanning part of the α and β protein subunits (Figure 1) arranged in high symmetry in the LH2 complex.

Of particular interest are distinct collections of peaks in the NCA spectrum (N_i–$C_{\alpha,i}$) at 42–46 ppm and 47–49 ppm ^{13}C chemical shift. Based on their characteristic ^{13}C chemical shifts, these correlations can be type-assigned to Gly and Ala residues, respectively. In addition, C_α resonances of Pro residues can be tentatively assigned at 63.2 and 63.6 ppm in Figure 5B. As expected for a band-selective experiment, for both Pro residues we observe C_δ resonances (Figure 5B) and correlations of type N_iCO_{i-1} in Figure 5A. Note that an additional weaker NC_α-type correlation is observed (147 ppm, 62.5 ppm) with a significantly larger line width in the ^{15}N dimension. As discussed in more detailed below, both observations would be consistent with the detection of a third Pro residue in C-terminal portions of the LH2 membrane protein (Figure 1). The chemical shift statistics obtained in the liquid state (Wishart et al., 1991) for particular amino acid residues suggest additional spectral regions which are consistent with the experimental results. Such annotations are included for Val, Ile, Ser and Thr C_α correlations in Figure 5B. They do not represent spectral assignments but will be useful for the analysis presented in the following.

2D (NCC) correlation experiments

Additional information can be obtained if the NC correlations presented so far are combined with a homonuclear polarization transfer element. In the current context, we have relied on the mechanism of homonuclear spectral spin diffusion ('SD', Bloembergen, 1949), where polarization transfer among rare spin carbons is mediated by a strongly coupled proton bath. During the NMR experiment, SD mediated transfer is achieved by insertion of a longitudinal mixing time $\tau(^{13}C,^{13}C)$ after the SPECIFIC CP transfer step and prior to detection in t_2 (Figure 4). Unlike coherent recoupling techniques (see e.g. Baldus et al., 1998a; Rienstra et al., 1998; Howhy et al., 1999), strong proton decoupling during mixing can be omitted.

In Figure 6, we present results of a 2D NCC correlation experiment in which band-selective NCA transfer is followed by a homonuclear SD mixing unit. In the initial rate regime of a homonuclear spin pair, proton-driven spin diffusion rates under MAS are dependent on the size of the MAS frequency ω_R and the isotropic chemical shift difference Δ. In particular, if the resonance condition $\Delta = n\omega_R$ (where n = 1, 2,...) is fulfilled, an enhanced transfer rate is expected (Kubo and McDowell, 1988). For 8 kHz MAS at 750 MHz, an SD mixing time $\tau(^{13}C,^{13}C)$ of 8 ms is sufficient to observe one-bond correlations. Polarization transfer across two bonds is influenced by the resonance condition discussed above. In general, the combination of a broadband HN and band-selective NC transfer also permits correlations within nitrogen-containing side chains. This is exemplified in Figure 6A, where correlations at 90 ppm ^{15}N chemical shift are observed. Inspection of the primary sequence (Figure 1) predicts only one Arg side-chain correlation at residue 20 of the β apoprotein. The observed

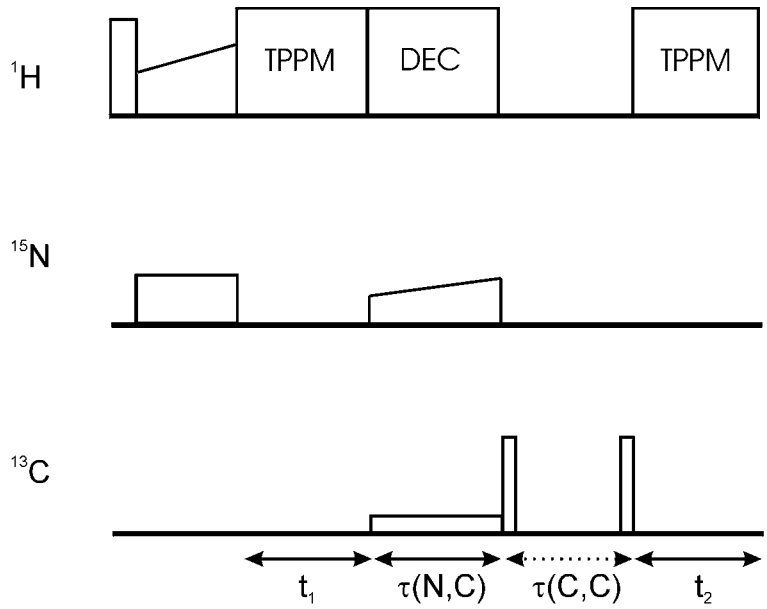

Figure 4. Triple channel (^{1}H,^{15}N,^{13}C) pulse scheme to observe ^{15}N,^{13}C correlations in two dimensions. Following a broadband (^{1}H,^{15}N) ramped CP transfer of 2 ms, ^{15}N chemical shift evolution under TPPM decoupling at 85 kHz r.f. field strength occurred during t_1. Subsequently, a SPECIFIC CP (Baldus et al., 1998b) transfer step was used to establish NC transfer for a ^{13}C chemical shift range of 20–30 ppm around the carrier frequency. Band-selectivity was achieved using linear (100% − X%, X = 70 or 80) amplitude modulations on the ^{15}N channel. It should be noted that other amplitude modulations (Hediger et al., 1995) are also possible. During dipolar contact, maximum ^{15}N and ^{13}C r.f. fields of 25 and 15 kHz, respectively, were employed. All 2D experiments were performed at −10 °C using a MAS frequency of 8 kHz and a heteronuclear transfer time τ(^{15}N,^{13}C) of 2 ms. During (NC) transfer, the decoupling efficiency was optimized by off-resonance CW irradiation (Baldus et al., 1996) and switched back to on-resonance conditions for the remainder of the sequence. Homonuclear polarization transfer for the 2D (NCC) correlations shown in Figures 6 and 7 was achieved by insertion of a proton-driven spin diffusion transfer unit prior to acquisition in t_2. Bracketed by two 90° pulses (using r.f. fields of 50 kHz), residual proton-proton and proton-carbon dipolar couplings are active for the mixing time τ(^{13}C,^{13}C). Phase sensitive detection was achieved using the TPPI method (see e.g. Ernst et al., 1987).

^{15}N chemical shift of 90 ppm agrees well with average chemical shifts observed in soluble proteins and is consistent with model studies involving Arg containing peptides (Baldus et al., unpublished results). We thus assign the two correlations to $R_{20\delta}$ (56.2 ppm) and $R_{20\gamma}$ (31.6 ppm). Moreover, we could also identify the correlations to $R_{20\varepsilon}$ and $R_{20\zeta}$ (at 157.3 ppm and 32 ppm respectively, data not shown), and a weaker correlation at 28.5 ppm indicative for the observation of $R_{20\beta}$.

Hence, heteronuclear polarization transfer from the guanidyl group allows for the identification of the R20 residue and can be validated by investigating signal intensities originating from the amide backbone. In Figure 6, this has been carried out by drawing vertical lines from the C_β and C_γ correlations observed in Figure 6A into the $C_\alpha C_\beta C_\gamma$ region of the experiment (Figure 6B). For both ^{13}C shifts we expect a horizontal correlation representing the C_α, C_β, and C_γ resonances of R20 tentatively assigned in Figure 6B. Moreover, the observed correlation allows for an internal calibration of the signal intensity of an individual NC or CC correlation in the presented spectra.

Using the intensity information for the Arg residue, at least 4 Gly correlations are observable. Thr residues are often characterized by C_β chemical shifts well above 60 ppm and C_γ correlations around 20 ppm (Wishart al., 1991). As indicated in Figure 6B, we observe at least three sets of Thr $C_{\alpha-\gamma}$ correlations for ^{15}N chemical shift values of 107–111 ppm. Albeit significant variations in signal intensities, this number matches the number of membrane-spanning Thr residues. Discrimination between Ser and Thr peaks can be attempted using their different side-chain topologies. As a result, 2–3 Ser correlations can be identified and are indicated in Figure 6B. In line with recent observations in immobilized globular proteins (McDermott et al., 2000; Pauli et al., 2001) the observed ^{13}C chemical shifts compare favorably with observations in the liquid state. On the other hand, the observed ^{15}N chemical shift values deviate by about

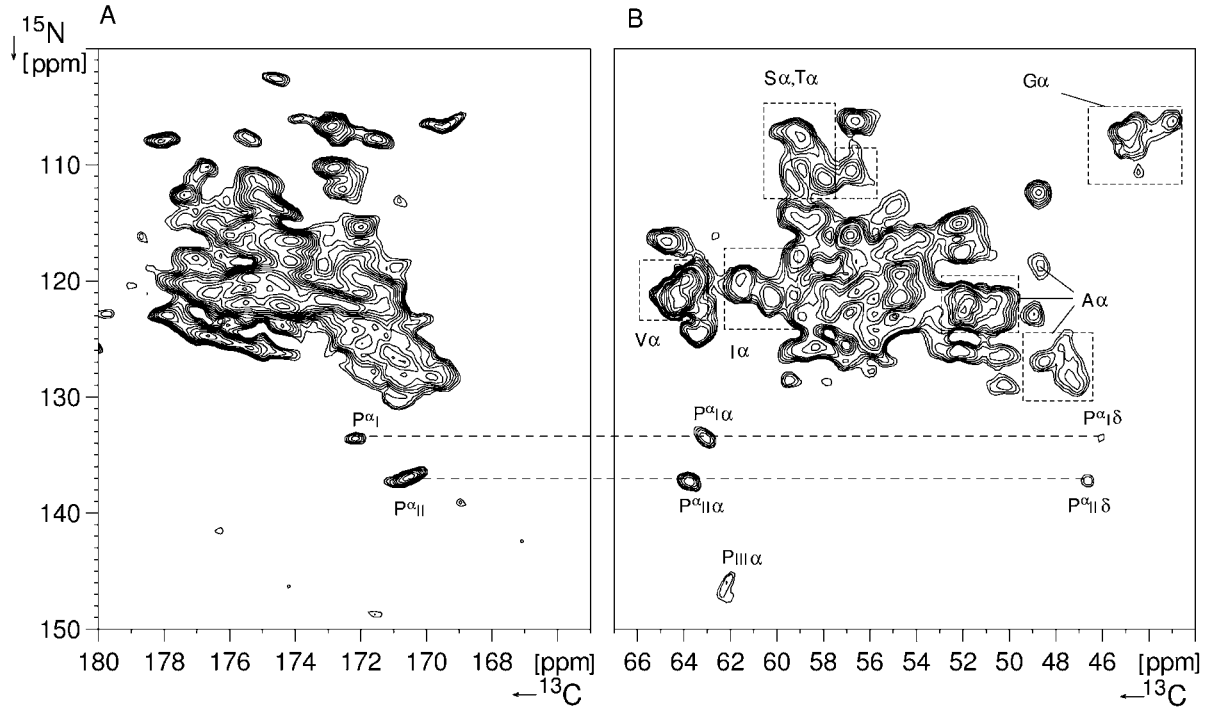

Figure 5. Heteronuclear (N,C) correlation spectra obtained on [U-^{13}C,^{15}N] LH2. In A and B, the ^{13}C carrier frequency was placed slightly outside the CO and C_α region of the ^{13}C spectrum, respectively. Band-selective SPECIFIC CP transfer around the $n = 1$ condition discussed in the text was optimized using the experimental setup of Figure 4. In both cases, 128 t_1 points were accumulated. For backbone resonances, correlations of type ($N_i CO_{i-1}$, Figure 5A) and $N_i C_{\alpha i}$ (Figure 5B) are expected. Results from liquid-state NMR data (Wishart et al., 1991) are used to identify the C_α resonance areas of the amino acids S, T, G, V, I, and P. In total, three (I–III) correlations involving P residues are detected. For the two stronger sets of signals additional C_δ and CO resonances of the P residue and its preceding amino acids, respectively, can be identified and are attributed to the membrane-spanning segments in apoprotein α. For the S, T, G, V and I residues, dashed boxes are used to annotate possible correlation areas. They do not represent spectral assignments.

5 ppm from the average shifts observed in globular proteins (Wishart et al., 1991).

Additional correlations around and below 20 ppm may result from Ala and Ile residues. In total we expect 14 correlations for both types of amino acids in the membrane-spanning segment. Using information on the characteristic side-chain chemical shift, at least one set of $A_{\alpha,\beta}$ and $I_{\alpha-\gamma 2}$ correlations at 115 and 119 (^{15}N) ppm, respectively, can be identified. Possible additional correlation areas as indicated in Figure 6B can be defined. Comparison between Figures 6A and 6B indicates that correlations around 15–20 ppm are in general stronger than for the $R_{20\beta}$ peak discussed earlier. This might partially be attributed to the resonance phenomenon mentioned earlier that favors C_α–C_γ polarization transfer across 40 ppm. Moreover, characteristic ^{15}N chemical shifts of Pro residues help to identify two sets of Pro resonances, as expected from the membrane-spanning portion of the protein. Two-bond C_β and C_γ correlations are clearly visible and agree with the NCA results of Figure 5B. Finally, areas consistent with average chemical shift values for Val_α, Ile_α, Ile_α and $Val_{\gamma 1}$ correlations are given in Figure 6. Again, they do not represent spectral assignments.

Interresidue connectivities can be established by combining the information obtained so far with results of an N_i-$(COC_\alpha C_\beta)_{i-1}$ experiment (Figure 7). In the present context, we will attempt to establish preliminary interresidue contacts for residues containing characteristic chemical shifts to illustrate the principle of sequence-specific assignment under MAS for a membrane-protein complex. The limited chemical shift range in the CO part of the spectrum does, for most cases, not permit to resolve individual correlations. However, the NCO transfer serves as a relay step to observe characteristic side-chain topologies of the preceding residue in the polypeptide chain. Since analogous experimental conditions were employed as in Figure 6, correlation patterns of the form CO-C_α-C_β are to be expected. The combination of a broad-

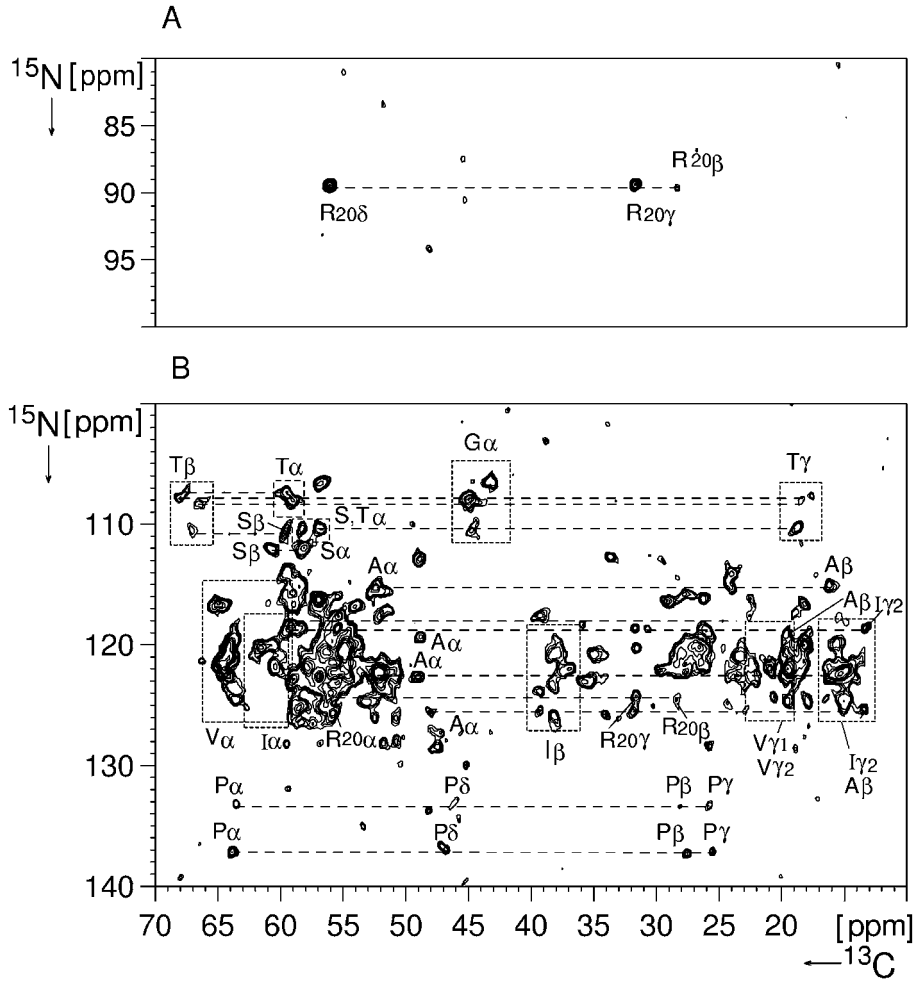

Figure 6. Combined NC-CC 2D transfer experiment on [U-^{13}C,^{15}N] LH2 that reveals side chain–side chain (A) and backbone–side chain (B) N-C-C correlation patterns. As a preparatory step, SPECIFIC CP transfer was used to isolate carbon resonances around 50 ppm. A subsequent spin diffusion time τ(CC) of 8 ms allows for transfer along two additional peptide bonds of type $C_\alpha C_\beta C_\gamma$. In (A) side-chain resonances of residue R are identified. In B, various correlation sets in the backbone region of the experiment are indicated by horizontal lines and are discussed in the text. Further information regarding the annotations is given in the text. In analogy to Figure 5, dashed boxes indicate possible correlation areas for various amino acids.

band HN and band-selective NC transfer here also permits correlations of the form C_δ-C_γ-C_β and C_γ-C_β-C_α for Q (Gln) and N (Asn) residues, respectively. However, both amino acids do not occur within the membrane-spanning section of the protein.

In Figure 7, where the aliphatic region of the N-CO-C_α-C_β-type experiment is shown, one of the four interresidue correlations involving G residues of the β protein subunit can be immediately identified ($G^{18}T^{19}$). Likewise, tentative assignments for the pairs $G^{15}I^{16}$, $G^{21}S^{22}$ of the α-apoprotein and $G^{24}L^{25}$ of the β-apoprotein in the membrane-spanning part are included. Following the discussion presented earlier, correlations observed around 20 ppm should predominately arise from A (Ala) residues. Distinct sets of chemical shifts should thus be detectable for the two AT pairs of the protein, namely the $A^{36}T^{37}$ pair at the end of the membrane-spanning part and A^1T^2 at the N-terminus of the β-protein segment. One correlation is readily identified in Figure 7. In line with the results presented so far it seems probable that stronger signals result from polarization transfer among membrane-spanning residues and we consequently assign this correlation to the pair $A^{36}T^{37}$. Following the same argumentation we can now also resolve the ambiguity of the two P resonances observed in Figures 5 and

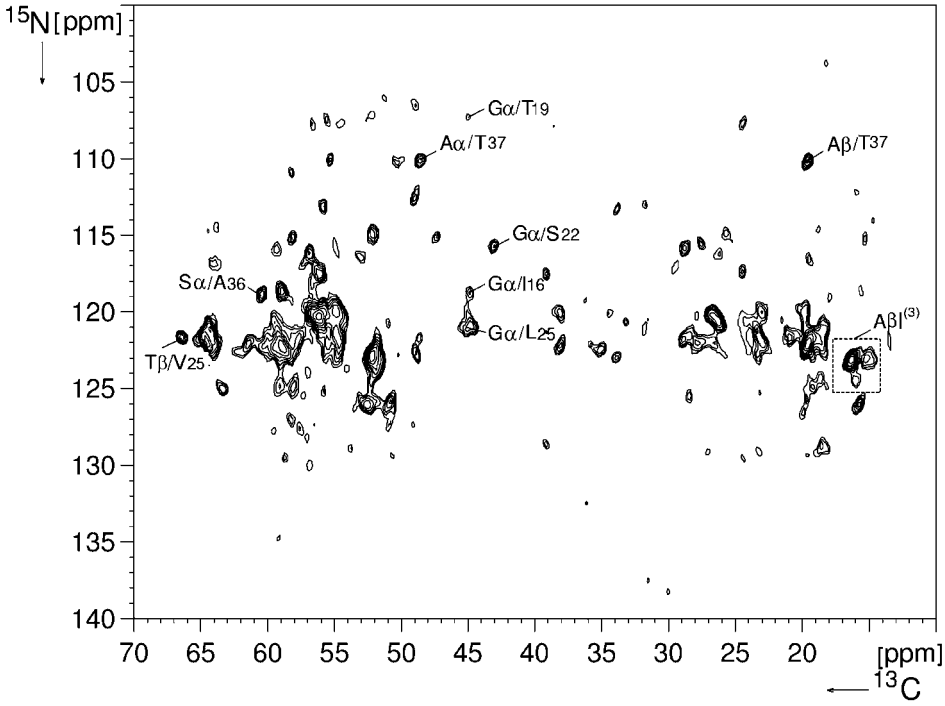

Figure 7. Combined NC-CC 2D transfer experiment on [U-^{13}C,^{15}N] LH2. The experimental setup differs from Figure 6 by SPECIFIC CP transfer tailored to CO resonances around 178 ppm (under identical parameters as in Figure 5A). A subsequent spin diffusion time τ(CC) of 8 ms allows for transfer along two additional peptide bonds of the type CO-$C_\alpha C_\beta$. The $C_\alpha C_\beta$ segment of the experiment containing the largest dispersion is shown. Four correlations involving G residues are assigned. Likewise, A- or T-containing residue pairs (i,i+1) are indicated in the form $S(C_{\alpha i})/A_{i+1}$, $T(C_{\beta i})/V_{i+1}$ and $A(C_{\alpha,\beta i})/T_{i+1}$. Finally a correlation area for three pairs of the form $A_i I_{i+1}$ is given.

6 and we assign the set of stronger signals to P17, deeply embedded in the membrane. Figure 7 also contains a tentative assignment of the $A_\alpha{}^{36}T^{37}$ peak that is consistent with the results of Figure 6. Characteristic chemical shifts also allow for the assignment of the pair $S^{35}A^{36}$ and for the identification of a T_β correlation at 66 ppm that could be consistently extended to the $T^{24}V^{25}$ pair of the α-apoprotein. Figure 7 indicates the occurrence of at least four more AX pairs, in close agreement with 3 AI, 2 AL and one AF pair in the membrane. Using the information in Figure 6, three AI pairs are tentatively identified. Obviously, additional information is needed to completely assign these segments.

The protein residues discussed in this work are summarized in Figure 1 by underlined letters. Except for the three AI pairs and one S residue for which we can currently only give a classification by type (see Figure 7), all indicated residues have been spectrally assigned (indicated by a line above the letter) and are summarized in Table 1 of the Appendix. As expected, we also observe two proline resonances in the CO portion of Figure 7 (data not shown). For both residues, however, proton driven polarization transfer to the CACB region of the spectrum is weak. Similar observations were recently made (Pauli et al., 2001) in an immobilized globular protein, indicative of an additional influence of the proton density at a given residue during SD polarization transfer. Additional experiments, e.g. involving coherent homonuclear transfer elements (see e.g. Baldus et al., 1998a; Rienstra et al., 1998; Howhy et al., 1999), might clarify this issue and provide complementary intra- and inter-residue information.

Conclusions

The data presented so far show that even at low temperatures and with MAS significant resolution in 2D correlation spectra of a uniformly labeled membrane-protein can be obtained. A preliminary analysis of distinct amino acid residues indicates that significant portions of the membrane-spanning section can be detected. On the other hand, backbone and side-chain

correlations involving N and C terminal loop segments of the protein appear to be significantly attenuated. Similar effects have recently been observed in immobilized globular proteins (Pauli et al., in press). In the chosen temperature regime, flexible portions of the protein could be frozen in a variety of different conformations giving rise to a relatively broad background signal (VanderHart et al., 1981; Fischer et al., 1992). Alternatively, enhanced flexibility, even at the temperatures employed, could lead to smaller dipolar couplings that attenuate the polarization transfer efficiency for flexible protein sections.

The observation of an additional Pro residue outside the membrane-spanning part of the α-apoprotein could indicate that also residues of defined secondary structure outside the membrane (such as P^{21} of the surface-bound helical segment; McDermott et al., 1995) can in principle be detected. The observation of the alpha-helical membrane-spanning parts of the protein would also be consistent with the limited chemical shift ranges in the recorded NC correlations. Although the latter argument is usually employed in the context of liquid state NMR applications, preliminary results in immobilized globular proteins (Pauli et al., 2001) and oriented systems (Marassi and Opella, 1998) indicate the validity also in the solid state. Additional experiments, e.g. involving variable dipolar contact times or methods that are sensitive to secondary structure elements, will clarify these issues.

Moreover, experiments e.g. involving coherent (^{13}C,^{13}C) transfer steps, three-dimensional correlation spectroscopy or the incorporation of heteronuclear NC (spin-spin) decoupling schemes should enable a more detailed analysis. Our current study resulted in the detection of about 40% of the trans-membrane segments of the protein. Although the observed line width is likely mostly dominated by heterogeneous broadening effects, additional line narrowing might result from higher spinning speeds or stronger proton decoupling fields. Additional information could be obtained from Multi-Quantum experiments or spectral editing and filtering experiments that simplify the spectral analysis significantly. A subsequent structure elucidation might also profit from long-range proton-proton transfer or torsional constraints. Similar routes are currently investigated in oriented liquid-state NMR systems (Tjandra and Bax, 1997; Prestegard, 1998). Finally, varying experimental conditions such as temperature, the degree of sample labeling or the choice lipid/detergent environment can be explored to improve the resolution.

Experiments along these lines are currently ongoing in our laboratory and will be reported elsewhere. The data obtained so far hold promise that SSNMR-related studies of ligand-binding interactions in membrane-proteins involving small to medium size polypeptides should be feasible. The results obtained so far also indicate that MAS-based correlation experiments might complement structural studies in multiply labeled membrane-proteins where macroscopic orientation techniques suffer from decreased spectral resolution (Marassi et al., 2000). Both approaches contribute to the converging evidence that solid-state NMR can reveal structural information in biophysical systems that are not accessible by other spectroscopic methods at present.

Acknowledgements

This project was financed in part by demonstration project BI04-CT97-2101 of the commission of the European communities. H.J.M.dG. is a recipient of a PIONIER award of the Chemical Sciences section of the Nederlandse Organisatie voor Wetenschappelijk Onderzoek (CW-NWO). Support from D. de Wit and C. Erkelens during various stages of the project is gratefully acknowledged. We thank S. Luca for carefully reading the manuscript.

Appendix

Summary of protein resonances assigned in this work

Residue	NH (ppm)	Cα (ppm)	Cβ (ppm)	Cγ (ppm)	Cδ (ppm)
P12	133.4	63.1	27.9	26.0	46.0
G15	107.8	45.0			
I16	118.8	59.1	31.6	30.5	14.0 (γ2)
P17	137.0	63.8	27.5	25.6	46.5
G21	106.8	43.8			
S22	115.5	58.2	56.8		
T24	108.4	58.0	66.8	18.2	
V25	121.8	64.8			
G18	107.5	44.9			
T19	107.3	59.5	67.2	17.8	
R20	124.5	56.4	28.5	31.6	56.2
G24	110.5	45.1			
L25	121.2				
S35	114.5	60.2			
A36	118.8	48.2	19.5		
T37	109.9	57.6	67.1	19.5	

References

Andrew, E.R., Bradbury, A. and Eades, R.G. (1958) *Nature*, **182**, 1659.

Baldus, M., Geurts, D.G., Hediger, S. and Meier, B.H. (1996) *J. Magn. Reson.*, **A118**, 140–144.

Baldus, M., Geurts, D.G. and Meier, B.H. (1998a) *Solid-state NMR*, **11**, 157–168.

Baldus, M., Petkova, A.T., Herzfeld, J. and Griffin, R.G. (1998b) *Mol. Phys.*, **95**, 1197–1207.

Bennett, A.E., Griffin, R.G. and Vega, S. (1994) *NMR Basic Principles Progr.*, **33**, 1–77.

Bennett, A.E., Rienstra, C.M., Auger, M., Lakshmi, K.V. and Griffin, R.G. (1995) *J. Chem. Phys.*, **103**, 6951–6958.

Benzinger, T.L.S., Gregory, D.M., Burkoth, T.S., Miller-Auer, H., Lynn, D.G., Botto, R.E. and Meredith, S.C. (1998) *Proc. Natl. Acad. Sci. USA*, **95**, 13407–13412.

Bloembergen, N. (1949) *Physica*, **15**, 386–426.

Boender, G.J., Raap, J., Prytulla, S., Oschkinat, H. and de Groot, H.J.M. (1995) *Chem. Phys. Lett.*, **237**, 502–508.

Bower, P.V., Oyler, N., Mehta, M.A., Long, J.R., Stayton, P.S. and Drobny, G.P. (1999) *J. Am. Chem. Soc.*, **121**, 8373–8375.

Cavanagh, J., Fairbrother, W.M., Palmer, A.G. and Skelton, N.J. (1996) *Protein NMR Spectroscopy: Principles and Practice*, Academic Press, San Diego, CA.

Creuzet, F., McDermott, A., Gebhard, R., van der Hoef, K., Spijker-Assink, M.B., Herzfeld, J., Lugtenburg, J., Levitt, M.H. and Griffin, R.G. (1991) *Science*, **251**, 783–786.

Cross, T.A. and Opella, S.J. (1994) *Curr. Opin. Struct. Biol.*, **4**, 574–581.

Egorova-Zachernyuk, T.A., van Rossum, B., Boender, G.J., Franken, E., Ashurst, J., Raap, J., Gast, P., Hoff, A.J., Oschkinat, H. and de Groot, H.J.M. (1997) *Biochemistry*, **36**, 7513–7519.

Ernst, R.R., Bodenhausen, G. and Wokaun, A. (1987) *Principles of Nuclear Magnetic Resonance in One and Two Dimensions*, Clarendon Press, Oxford.

Feng, X., Verdegem, P.J.E., Lee, Y.K., Sandstrom, D., Eden, M., Bovee-Geurts, P., de Grip, W.J., Lugtenburg, J., de Groot, H.J.M. and Levitt, M.H. (1997) *J. Am. Chem. Soc.*, **119**, 6853–6857.

Feng, X., Verdegem, P.J.E., Lee, Y.K., Sandstrom, D., Eden, M., Bovee-Geurts, P., de Grip, W.J., Lugtenburg, J., de Groot, H.J.M. and Levitt, M.H. (2000) *J. Biomol. NMR*, **16**, 1–8.

Fischer, M.R., de Groot, H.J.M., Raap, J., Winkel, C., Hoff, A.J. and Lugtenburg, J. (1992) *Biochemistry*, **31**, 11038–11049.

Griffin, R.G. (1998) *Nat. Struct. Biol.*, **5**, 508–512.

Griffiths, J.M., Lakshmi, K.V., Bennett, A.E., Raap, J., Van der Wielen, C.M., Lugtenburg, J., Herzfeld, J. and Griffin, R.G. (1994) *J. Am. Chem. Soc.*, **116**, 10178–10181.

Hawthorn, A.M. and Cogdell, R.J. (1991) In *Chlorophylls* (Ed., Scheer, H.), CRC Press, Boca Raton, FL, pp. 493–528.

Hediger, S., Meier, B.H. and Ernst, R.R. (1995) *Chem. Phys. Lett.*, **240**, 449–456.

Hohwy, M., Rienstra, C.M., Jaroniec, C.P. and Griffin, R.G. (1999) *J. Chem. Phys.*, **110**, 7983–7992.

Hong, M. (1999) *J. Biomol. NMR*, **15**, 1–14.

Hong, M. and Jakes, K. (1999) *J. Biomol. NMR*, **14**, 71–74.

Kay, L.E., Ikura, M., Tschudin, R. and Bax, A. (1990) *J. Magn. Reson.*, **89**, 496–514.

Ketchem, R.R., Hu, W. and Cross, T.A. (1993) *Science*, **261**, 1457–1460.

Ketchem, R.R., Roux, B. and Cross, T.A. (1997) *Structure*, **5**, 1655–1669.

Klug, C.A., Tasaki, K., Tjandra, N., Ho, C. and Schaefer, J. (1997) *Biochemistry*, **36**, 9405–9408.

Kubo, A. and McDowell, C.A. (1988) *J. Chem. Soc., Faraday Trans.*, **84**, 3713–3730.

Marassi, F.M. and Opella, S.J. (1998) *Curr. Opin. Struct. Biol.*, **8**, 640–648.

Marassi, F.M., Ma, C., Gratkowski, H., Straus, S.K., Strebel, K., Oblatt-Montal, M., Montal, M. and Opella, S.J. (1999) *Proc. Natl. Acad. Sci. USA*, **96**, 14336–14341.

Marassi, F.M., Ma, C., Gesell, J. and Opella, S.J. (2000) *J. Magn. Reson.*, **144**, 156–161.

McDermott, A., Polenova, T., Bockmann, A., Zilm, K.W., Paulsen, E.W., Martin, R.W. and Montelione, G.T. (2000) *J. Biomol. NMR*, **16**, 209–219.

McDermott, G., Prince, S.M., Freer, A.A., Hawthorn-Lawless, A.M., Paiz, M.Z., Cogdell, R.J. and Isaacs, N.W. (1995) *Nature*, **374**, 517–521.

McDowell, L.M. and Schaefer, J. (1996) *Curr. Opin. Struct. Biol.*, **6**, 624–629.

Mehring, M. (1983) *Principles of High Resolution NMR in Solids*, Springer Verlag, Berlin.

Metz, G., Wu, X.L. and Smith, S.O. (1994) *J. Magn. Reson.*, **110**, 209–227.

Montelione, G.T. and Wagner, G. (1990) *J. Magn. Reson.*, **87**, 183–188.

Nomura, K., Takegoshi, K., Terao, T., Uchida, K. and Kainosho, K. (1999) *J. Am. Chem. Soc.*, **121**, 4064–4065.

Opella, S.J., Marassi, F.M., Gesell, J.J., Valente, A.P., Kim, Y., Oblatt-Montal, M. and Montal, M. (1999) *Nat. Struct. Biol.*, **6**, 374–379.

Pauli, J., Baldus, M., van Rossum, B., de Groot, H.J.M. and Oschkinat, H. (2001): *Chem. BioChem.*, in press.

Pellegrini, M. and Mierke, D.F. (1999) *Biopolymers (Pept. Sci.)*, **51**, 208–220.

Pines, A., Gibby, M.G. and Waugh, J.S. (1973) *J. Chem. Phys.*, **59**, 569–590.

Prestegard, J.H. (1998) *Nat. Struct. Biol.*, **5**, 517–522.

Rienstra, C.M., Hatcher, M.E., Mueller, L.J., Sun, B., Fesik, S.W. and Griffin, R.G. (1998) *J. Am. Chem. Soc.*, **120**, 10602–10612.

Sanders, C.R., Hare, H.J., Howard, K.P. and Prestegard, J.H. (1994) *Prog. NMR Spectrosc.*, **26**, 421–444.

Siegal, G., van Duynhoven, J. and Baldus, M. (1999) *Curr. Opin. Chem. Biol.*, **3**, 530–536.

Smith, S.O., Aschheim, K. and Groesbeek, M. (1996) *Quart. Rev. Biophys.*, **29**, 395–449.

Straus, S.K., Bremi, T. and Ernst, R.R. (1998) *J. Biomol. NMR*, **12**, 39–50.

Thompson, L.K., McDermott, A.E., Raap, J., van der Wielen, C.M., Lugtenburg, J., Herzfeld, J. and Griffin, R.G. (1992) *Biochemistry*, **31**, 7931–7938.

Tjandra, N. and Bax, A. (1997) *Science*, **278**, 1111–1114.

VanderHart, D.L., Earl, W.L. and Garroway, A.N. (1981) *J. Magn. Reson.*, **44**, 361–401.

Verdegem, P.J.E., Bovee-Geurts, P.H.M., de Grip, W.J., Lugtenburg, J. and de Groot, H.J.M. (1999) *Biochemistry*, **38**, 11316–11324.

Watts, A. (1999) *Curr. Opin. Biotechnol.*, **10**, 48–53.

Wishart, D.S., Sykes, B.D. and Richards, F.M. (1991) *J. Mol. Biol.*, **222**, 311–333. For a recent statistical compilation of chemical shifts in proteins, see also: Biomolecular NMR Data Bank (BioMagResBank): A Repository for Data from NMR Spectroscopy on Proteins, Peptides, and Nucleic Acids, http://www.bmrb.wisc.edu/

Zuber, H. and Brunisholz, R.A. (1993) In *The Chlorophylls* (Ed., Scheer, H.), CRC Press, Boca Raton, FL, pp. 627–692.